Modulation of NF-κB-dependent gene transcription using programmable DNA minor groove binders

Jevgenij A. Raskatov[a], Jordan L. Meier[a], James W. Puckett[a], Fei Yang[a], Parameswaran Ramakrishnan[b], and Peter B. Dervan[a,1]

[a]Division of Chemistry and Chemical Engineering and [b]Division of Biology, California Institute of Technology, Pasadena, CA 91125

Contributed by Peter B. Dervan, November 10, 2011 (sent for review September 14, 2011)

Nuclear factor κB (NF-κB) is a transcription factor that regulates various aspects of immune response, cell death, and differentiation as well as cancer. In this study we introduce the Py-Im polyamide 1 that binds preferentially to the sequences 5′-WGGWWW-3′ and 5′ GGGWWW-3′. The compound is capable of binding to κB sites and reducing the expression of various NF-κB–driven genes including *IL6* and *IL8* by qRT-PCR. Chromatin immunoprecipitation experiments demonstrate a reduction of p65 occupancy within the proximal promoters of those genes. Genome-wide expression analysis by RNA-seq compares the DNA-binding polyamide with the well-characterized NF-κB inhibitor PS1145, identifies overlaps and differences in affected gene groups, and shows that both affect comparable numbers of TNF-α–inducible genes. Inhibition of NF-κB DNA binding via direct displacement of the transcription factor is a potential alternative to the existing antagonists.

gene regulation | small molecule | plasminogen activator inhibitor 1

NF-κB encompasses a family of transcription factors that play a pivotal role in the inflammatory response, cell proliferation, and survival (1). It has been broadly implicated in cancer (2) and is a major contributor towards cellular senescence (3). The regulatory network of NF-κB has been studied at a high level of detail since its original discovery (4). Briefly, in the absence of stimulus such as tumor necrosis factor α (TNF-α), lipopolysaccharide, or interleukin 1 (IL1), NF-κB is sequestered in the cytosol in its inactive form, complexed to the inhibitory proteins of the IκB family. An induction signal leads to the activation of the IκB kinase complex (IKK), which targets the inhibitor proteins for ubiquitylation and proteasome-mediated degradation. The unmasked NF-κB proteins subsequently translocate into the cell nucleus, bind their target DNA sequences, termed κB sites (GGG*RNYYY*CC, where R = purine, Y = pyrimidine, and N = any base) and activate various gene programs, depending on the stimulus nature (5). The central biological importance of this transcription factor family together with its detailed structural and functional understanding makes it a particularly attractive drug target. A plethora of NF-κB inhibitors has been developed, which target different portions of the regulatory circuit (6). NF-κB regulates a vast number of cell processes, and its knockdown can have detrimental effects. It would therefore be useful to develop a strategy with which the expression of gene subgroups could be modulated while leaving the transcription factor itself intact.

Our laboratory has developed pyrrole-imidazole (Py-Im) polyamides as a class of modular DNA minor groove binders with affinities and specificities comparable to those of DNA-binding proteins (7–10). The minor groove binding of the DNA leads to the compression of the major groove that antagonizes transcription factor binding to the DNA major groove in an allosteric fashion (11). To date, they have been successfully applied in cell culture experiments to modulate the activity of the hypoxia inducible factor 1α, the androgen receptor, and the glucocorticoid receptor by our laboratory (12–15). Displacement of NF-kB by polyamides was also shown by electrophoretic mobility shift assays (16, 17). Matsuda and co-workers independently demonstrated that a Py-Im polyamide could be used to target the TGF-β promoter (18). Small molecule inhibitors mostly act upstream of the NF-κB DNA-binding event. They typically interfere with either the release of the transcription factor from the IκB complex or the DNA-binding ability of NF-κB, which can lead to broad and undesired side effects. The use of polyamide-based drugs to selectively disrupt the NF-κB binding to a subset of κB sites without compromising the overall functionality of the transcription factor could represent an interesting alternative to the existing small molecule inhibitors.

Results

NF-κB ChIP-seq. ChIP-seq experiments with a p65-specific antibody were conducted to gain better understanding of NF-κB binding in cell culture (A549, human non-small lung carcinoma). The highest occupancy of the proximal promoters of the known NF-κB target genes *IL6* and *IL8* was observed after 30 min TNF-α induction (Fig. S1). This time point was therefore chosen for ChIP-seq experiments. The predominant binding motif was determined as *N*GG*NN*TTTCC*N* by an unbiased search (Fig. 1*A*), in good agreement with the recent study conducted for a panel of lymphoblastoid cell lines (19).

The determined sequence was employed to guide polyamide design, yielding the Py-Im polyamide **1** [ImImPyPy-$(R)^{\alpha\text{-amino}}{}_{\gamma}$-PyPyPyPy], specific for the DNA sequence 5′WGGWWW-3′ according to the pairing rules (10).

Py-Im Polyamide 1 Binds to the κB Sites within the *IL6* and *IL8* Promoter. Following the guidelines from the ChIP-seq experiment, the polyamide **1** capable of binding the sequence 5′-WGGWWW-3′ was synthesized (Fig. 1*B*). An initial set of DNA melting temperature analyses was conducted to assess the binding propensity of **1** towards the matched binding site (5′-WGGWWW-3′) as well as that bearing a single mismatch over the polyamide C terminus (5′GGGWWW-3′). These two sequences are found in a large number of κB sites and hence possess a biological significance. For our initial experiments, the genes *IL6* and *IL8* were chosen. Their NF-κB response elements (κB sites) possess the sequence 5′-GGGATTTTCCC-3′ (chr7:22,766,746-22,766,756) and 5′ GTGGAATTTCC-3′ (chr4:74,606,193-74,606,203), on the University of California Santa Cruz 2009 human genome browser (hg19), respectively (20, 21). In either of the κB sites, **1** is capable of binding in two orientations (Fig. 1*C*), which corresponds to the portions of the κB sites recognized by the p50 and the p65 subunit, respectively (1–5).

Author contributions: J.A.R. and P.B.D. designed research; J.A.R., J.L.M., and P.R. performed research; J.W.P. and F.Y. contributed new reagents/analytic tools; J.A.R., J.L.M., J.W.P., and P.R. analyzed data; and J.A.R. and P.B.D. wrote the paper.

The authors declare no conflict of interest.

Freely available online through the PNAS open access option.

Data deposition: The data reported in this paper have been deposited in the Gene Expression Omnibus (GEO) database, www.ncbi.nlm.nih.gov/geo (accession no. GSE34329).

[1]To whom correspondence should be addressed. E-mail: dervan@caltech.edu.

This article contains supporting information online at www.pnas.org/lookup/suppl/doi:10.1073/pnas.1118506109/-/DCSupplemental.

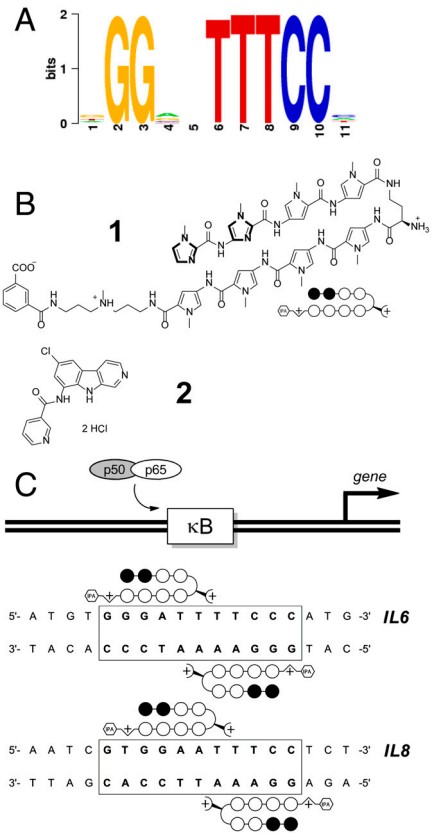

Fig. 1. (*A*) The NF-κB binding site determined by ChIP-seq. (*B*) The polyamide **1** and the IκB kinase inhibitor PS1145 **2**. (*C*) The targeted NF-κB response elements within the *IL6* and *IL8* promoter with the likely polyamide binding modes.

The DNA melting temperature was raised by 12.3(±0.6) °C (*IL6* κB site) and 10.7(±0.2) °C (*IL8* κB site) upon addition of **1**, thus indicating its significant binding to the two DNA sequences (Table 1, entries 1 and 4). Further oligonucleotides were designed to probe the binding of **1** to the fragments of the κB sites representing the p50 and p65 recognition elements (Table 1, entries 2–3 for *IL6* and 5–6 for *IL8*). The melting temperatures of the DNA duplexes experienced similar magnitudes of temperature increase upon polyamide addition. Quantitative DNase I footprint titration experiments of this Py-Im polyamide core have been previously reported by our laboratory ($K_a = 5 \times 10^8$ M^{-1}) (8).

Cellular Uptake of 1. The fluorescent FITC conjugate of **1** (**3**) was synthesized and its nuclear uptake studied in the A549 cell line (lung carcinoma). Robust reproducible cellular uptake was observed by confocal microscopy after 12–16 h incubation. Further evidence for cellular uptake of unmodified **1** was obtained by measuring compound cytotoxicity in live cells at different incubation time points (Fig. S2).

Table 1. Sequences used in the T_m analyses of 1

Entry	κB site	Sequence	T_m DNA	ΔT_m
1	*IL6*	5′-TGGGATTTTCCCAT-3′	55.1 (±0.3)	12.3 (±0.6)
2	$IL6_{P50}$	5′-TGTGGGATTTT-3′	47.3 (±0.1)	12.1 (±0.3)
3	$IL6_{P65}$	5′-ATTTTCCCATG-3′	44.0 (±0.3)	13.2 (±0.9)
4	*IL8*	5′-CGTGGAATTTCCTC-3′	56.4 (±0.1)	10.7 (±0.2)
5	$IL8_{P50}$	5′-TCGTGGAATTT-3′	46.2 (±0.5)	13.3 (±0.8)
6	$IL8_{P65}$	5′-GAATTTCCTCT-3′	43.7 (±0.6)	14.9 (±0.6)

T_m and ΔT_m values are reported in °C.

Inhibition of NF-κB Regulated *IL6* and *IL8* Expression. Encouraged by the favorable DNA-binding and cellular uptake properties of **1**, mRNA expression levels of *IL6* and *IL8* in response to polyamide treatment were investigated by qRT-PCR. Incubation of cells with **1** at a 10 μM concentration for 48 h, followed by a TNF-α stimulation for 12 h resulted in a significant reduction of both the *IL6* and *IL8* expression (Fig. 2*A*, 2.3-fold in both cases). The effects were more pronounced after 72 h incubation, the mRNA downregulation being 6.5-fold and 4-fold for *IL6* and *IL8*, respectively. Consistent transcript repression of both *IL6* and *IL8* was also seen at an earlier TNF-α induction time point (Fig. S3*A*). The expression levels of the housekeeping genes used [peptidylprolylisomerase A (PPIA) and glucuronidase, beta (GUSB)] remained stable upon treatment with **1**. The mRNA reduction correlated well with the protein levels as assessed by ELISA (Fig. S3*B*). In a control experiment we tested the effects of a κB-site mismatch polyamide by flipping the internal Im-Py pair of **1**, which would result in targeting of the 5′-WGCWWW-3′ sequence according to our DNA recognition rules. The relevant T_m analyses are summarized in Table S1. The effects of the resulting oligomer ImPyPyPy-$(R)^{\alpha\text{-amino}}\gamma$-PyPyImPy (**10**) on the expression of *IL6* and *IL8* were substantially lower as compared to **1**. A representative experiment is shown in Fig. S4 *A* and *B*. The ability of the scrambled polyamide to traffic to the nucleus of A549 was assessed by studying the uptake of its FITC-conjugate analog **11** (Fig. S4 *C* and *D*).

The ability of **1** to disrupt NF-κB binding to the characterized κB sites within the *IL6* and *IL8* promoters was examined by conducting ChIP-qPCR experiments on the corresponding genomic loci. The *IL6* promoter occupancy was reduced twofold upon polyamide treatment, whereas with *IL8* the effect was less pronounced with 1.5-fold reduction of promoter occupancy (Fig. 2*B*). Western blot analyses were conducted to assess the nuclear levels of p65 in response to the treatment with the Py-Im polyamide **1**. The compound was found not to affect the p65 trafficking to the nucleus in both uninduced (Fig. 2*C*) and TNF-α–induced (Fig. 2*D*) A549 cells. The use of the kinase inhibitor PS1145 led to the expected partial attenuation of TNF-α–induced p65 translocation in a control experiment (22).

Similarly to TNF-α, *IL1* can be used to activate the canonical NF-κB gene expression program (23). *IL1* signals through the cell surface receptor IL1R, employing a different signaling cascade upstream of NF-κB activation than TNF-α, which signals through the tumor necrosis factor receptor. However, both the *IL1* and the TNF-α stimulation ultimately result in the ubiquitylation of IκB inhibitory proteins, the translocation of the p50:p65 dimer into the nucleus, and the activation of canonical gene transcription. The Py-Im polyamide **1** being a DNA-binding molecule, one would anticipate that the difference in signaling upstream of NF-κB activation and nuclear translocation should not affect the effects of **1** on the expression of NF-κB–dependent genes. To this end, we assayed for the difference in expression of *IL6* and *IL8* upon treatment with the polyamide in a set of experiments where *IL1* was used as the inducing agent (Fig. 3). Paralleling the observations made in the TNF-α–induction experiments (Fig. 2*A* and Fig. S3*A*), we measured decreased levels of both *IL6* and *IL8* transcripts by qRT-PCR. Again, an incubation with **1** for 72 h prior to the *IL1* stimulation led to a more substantial repression of *IL6* (2.3-fold at 10 μM) and *IL8* (1.9-fold at 10 μM) than an incubation for 48 h (1.6-fold and 1.5-fold, respectively).

Genome-wide Polyamide Effects on TNF-α–Induced Gene Expression. Given the ability of **1** to down-regulate the mRNA expression of *IL6* and *IL8*, a series of RNA-seq experiments was conducted to establish the global effects of **1** on the TNF-α–inducible A549 transcriptome. The kinase inhibitor PS1145 (**2**) (Fig. 1*B*) was used as the reference molecule with a well-defined mechanism of action. A total of 979 genes (2.0% of the interrogated transcrip-

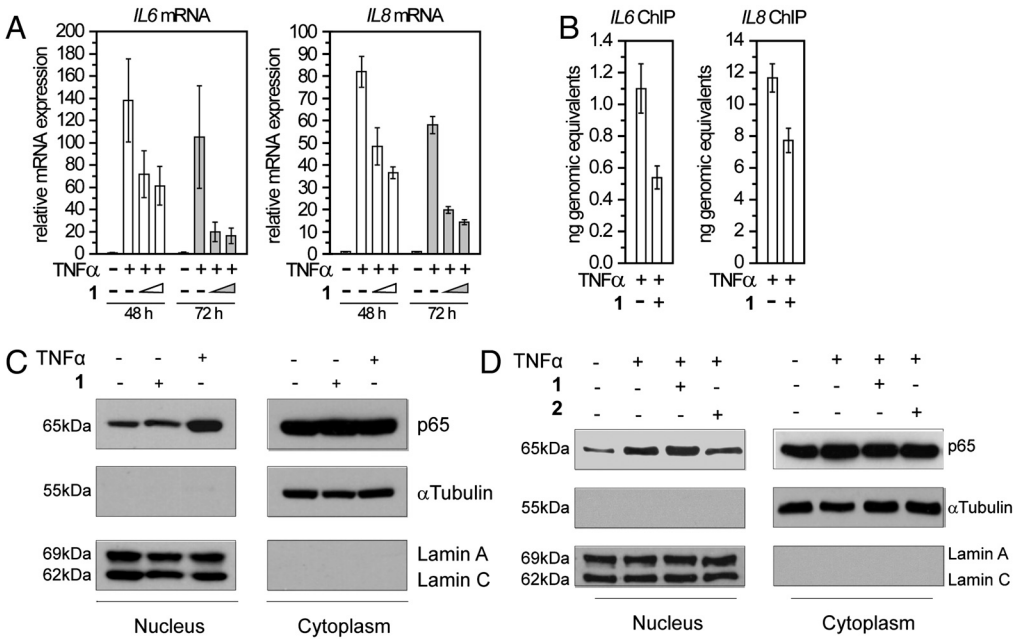

Fig. 2. (*A*) Changes in mRNA expression levels of *IL6* and *IL8* normalized to PPIA (48 or 72 h incubation with **1** at **5** or 10 μM, followed by an induction with TNF-α for 12 h, where indicated). (*B*) Genomic occupancy at the *IL6* and *IL8* proximal promoter (72 h incubation with **1** at 10 μM followed by an induction with TNF-α for 30 min). See Fig. S5 for further time course details. (*C*–*D*) Western blot analyses to assess cytoplasmic and nuclear p65 levels in response to the treatment with the Py-Im polyamide 1. A549 cells were incubated with 1 for 72 h and induced with TNF-α for 6 h, where indicated. Treatment with **2** was commenced 1.5 h prior to TNF-α induction. (*C*) Treatment with **1** does not alter basal nuclear p65 level. Nuclear (*Left*) and cytoplasmic (*Right*) extracts were analyzed for p65 protein levels. Purity of the nuclear and cytoplasmic extracts and normalization of loading were confirmed by probing for the nuclear protein lamin A/C and the cytoplasmic protein α-tubulin. (*D*) Treatment with **1** does not inhibit TNF-induced p65 nuclear translocation. Nuclear (*Left*) and cytoplasmic (*Right*) extracts were analyzed for p65 protein levels. **2** was used as a control for inhibition of TNF-α–induced p65 nuclear translocation. Purity of the nuclear and cytoplasmic extracts and normalization of loading were confirmed by probing for the nuclear protein lamin A/C and the cytoplasmic protein α-tubulin.

tome) had an expression change of more than twofold upon TNF-α stimulation. Within this subpopulation, 650 genes were up- and 329 down-regulated (Fig. 4 *A* and *B*). The polyamide **1** affected 1196 (2.4%) genes from which 671 were down-regulated with respect to the TNF-α stimulated reference. The kinase inhibitor **2** affected an approximately twofold smaller group of genes than the polyamide (613 genes, 1.2%, from which 332 were repressed).

From the 650 genes that were induced by TNF-α, only 67 were repressed by both **1** and **2** (Fig. 3*A*). In addition to those, 115 genes were found overlapping between TNF-α (up) and **1** (down) that were unaffected by **2**. Complementing that, there was an overlapping subgroup of 99 genes between TNF-α (up) and **2** (down) that was not affected by **1**. A large fraction of genes was found in nonoverlapping regions between the gene pools affected by TNF-α, **1** or **2**. From the 650 genes that were induced by

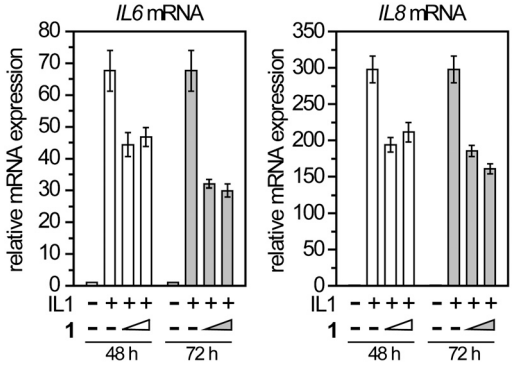

Fig. 3. Changes in mRNA expression levels of *IL6* and *IL8* normalized to PPIA (48 or 72 h incubation with **1** at 5 or 10 μM, followed by an induction with *IL1* for 2 h, where indicated).

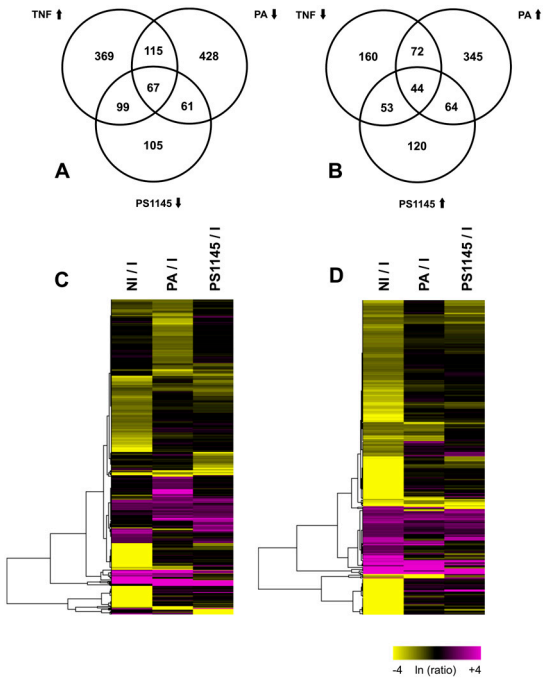

Fig. 4. RNA-seq global transcriptome analysis; all ratios are normalized to the induced state. (*A*) Venn diagrams for the overlap between TNF-α–induced genes and those repressed by **1** or **2** (all at least twofold). (*B*) Venn diagrams for the overlap between TNF-α–repressed genes and those induced by **1** or **2** (all at least twofold). (*C*) Hierarchical clustering (Euclidian distance, complete linkage) at least one change greater than fourfold per row. (*D*) Only genes changed greater than fourfold upon TNF-α stimulation were clustered (method the same as *C*). NI: noninduced, I: TNF-α–induced (12 h, 10 ng/mL). Treatment with **1** (72 h) or **2** (1.5 h) both at 10 μM final concentration.

TNF-α, 369 genes (56.8%) were not repressed by either **1** or **2**. The polyamide **1** repressed a total of 428 genes (63.8%) that were not induced by TNF-α or repressed by **2**. Finally, the kinase inhibitor **2** repressed a group of 105 genes (31.6%) that were neither induced by TNF-α nor repressed by **1**. Similar trends albeit with a smaller overall number of genes were seen for the intersection between TNF-α (up) **1** (down) and **2** (down). It has to be kept in mind that the TNF-α stimulation can lead to the activation of other regulatory circuits. The nonoverlapping sets between TNF-α, **1**, and **2** may stem from that to a degree.

Prior to conducting gene clustering analysis, more stringent filtering criteria were applied to the gene pool discussed above. Genes were kept where at least one fourfold change was observable upon TNF-α stimulation or treatment with either **1** or **2**. This procedure yielded a subset of 563 genes (Fig. 4*C*). A subgroup of those was furthermore projected out by applying the criterion of at least a fourfold change upon TNF-α treatment, yielding 314 genes overall (Fig. 4*D*). From the gene panel presented in Fig. 4*D*, 15 representative genes were selected that are known NF-κB targets (Fig. 5 *A*–*C*). Fig. 5*A* comprises five genes for which the effect of the polyamide **1** and the authentic inhibitor **2** are comparable, whereas in Fig. 5 *B* and *C* genes are displayed that are affected by **1** but not **2** and vice versa.

We confirmed the validity of the RNA-seq approach for quantitative transcriptome analysis by conducting qRT-PCR experiments on three representative genes from the panel displayed in Fig. 5 (*ICAM1*, *IL8*, and *SERPINE1*). High correlation was observed between the values obtained by the two techniques (Table 2). The corresponding bar graphs for the qRT-PCR control experiment are shown in Fig. S6.

Discussion

A large number of NF-κB inhibitors has been developed (6). They can be broadly classified as upstream or downstream inhibitors of NF-κB activity. The upstream inhibitors encompass molecules which affect various aspects of response initiation, the activity of the kinase complex IKK and the proteasome-mediated degradation of the NF-κB inhibitor proteins IκB. The downstream inhibitors comprise compounds with the ability to modulate NF-κB nuclear functions—i.e., its nuclear translocation, DNA binding, and transactivation. The main mode of action of the polyamide **1** is likely rooted in its DNA-binding properties and the resultant ability to displace transcription factors, which would place it downstream of NF-κB activation and potentially allow for a controlled regulation of a subgroup of the NF-κB regulatome.

Given the feedback regulation mechanism of NF-κB, response duration and magnitude can be affected. In order to shed light onto that aspect, the expression levels of the principal constituents of the NF-κB regulatory circuit (p50, p65, IκBα, β, and ε, and

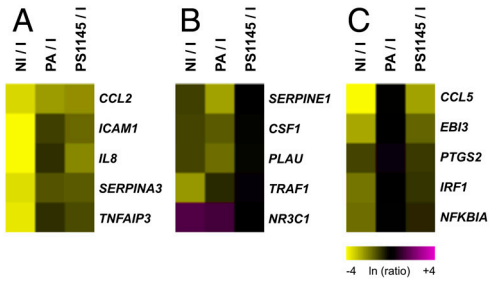

Fig. 5. (*A*) Known NF-κB targets that are induced by TNF-α and repressed by both **1** and **2**. (*B*) The noninduced state is partially restored by **1** but not **2**. (*C*) The noninduced state is partially restored by **2** but not **1**. NI: noninduced, I: TNF-α–induced (12 h, 10 ng/mL). Treatment with **1** (72 h) or **2** (1.5 h) both at 10 μM final concentration.

Table 2. Comparison of expression levels of *ICAM1*, *IL8*, and *SERPINE1* measured by RNA-seq (left) and qRT-PCR (right)

	RNA-seq		qRT-PCR	
Gene	Fold change 1	Fold change 2	Fold change 1	Fold change 2
ICAM1	2.9	5.2	3.8	5.7
IL8	2.3	8.4	2.7	7.0
SERPINE1	12.7	1.0	16.2	(1.1)

Treatment with **1** (72 h) or **2** (1.5 h) both at 10 μM final concentration. TNF-α induction (12 h, 10 ng/mL). Up-regulated genes have been put in brackets.

IKKα, β, and γ) were examined. Expression changes were substantially below twofold in most cases for both **1** and **2**.

The consensus binding sequence of NF-κB has been identified as 5′-GGG*RNYYY*CC-3′.(24) Our ChIP-seq experiments, conducted with an antibody against the p65 subunit, determined the binding motif to be 5′-*N*GG*NN*TTTCC*N*-3′. The first five base pairs represent a consensus superset of the p50 half-site (5′-*N*GG*NN*-3′ vs 5′-GGG*RN*-3′ in the consensus). The remaining portion of the NF-κB binding motif, the p65 half-site, was found to be substantially better defined (5′-TTTCC-3′ vs 5′-*YYY*CC-3′ in the consensus motif). The polyamide **1** can hence bind either the p50 half-site with one overhang into the p65 half-site (5′-*N*GG*NN*T-3′) or the reverse-complement of the p65 half-site with one additional base pair downstream (5′-*N*GGAAA-3′). Because of the overlap between the two potential binding sites, simultaneous binding of two polyamide molecules appears unlikely and the precise nature of the targeted binding sequence will determine which of the two half-sites is bound. Furthermore, in cellular context the affinities of the DNA for the polyamide **1** can be substantially altered because of the presence of higher order chromatin structures and further transcription factors bound to the DNA. The melting temperature analyses (Table 1) suggest that both the p50 and the p65 half-site within the two κB sites are fully capable of binding **1**. Given the difference in sequence between the oligonucleotides employed, quantitative comparisons between the ΔT_m values should be avoided.

The Py-Im polyamide **1** had comparable effects on *IL6* and *IL8* gene expression following the stimulation with both TNF-α and *IL1*. This finding can be interpreted as an indication that **1** is acting downstream of NF-κB activation and does not interfere with the cytosolic signaling cascades that lead to its activation. Given that the ChIP experiments demonstrated reduced p65 occupancy at both the *IL6* and *IL8* proximal promoter and the Western blot experiments showed that the polyamide does not impede nuclear trafficking of p65, the combined data are suggestive of a DNA-based mechanism of action for the Py-Im polyamide **1**.

The implication of the genome-wide transcriptome analysis (Fig. 4) is that the polyamide **1** possesses an acting profile that, although bearing a certain resemblance with the authentic NF-κB inhibitor **2**, also possesses its own distinct features. As such,

Table 3. Gene expression fold change upon polyamide treatment (up-regulated genes in brackets)

	A		B		C	
Gene	Fold change 1	Fold change 2	Gene	Fold change 1	Gene	Fold change 2
CCL2	11.8	9.8	*SERPINE1*	12.7	*CCL5*	13.6
ICAM1	2.9	5.2	*CSF1*	4.4	*EBI3*	5.0
IL8	2.3	8.4	*PLAU*	5.7	*PTGS2*	2.6
SERPINA3	4.1	4.2	*TRAF1*	2.1	*IRF1*	2.4
TNFAIP3	2.3	3.4	*NR3C1*	(3.3)	*NFKBIA*	2.0

A: Genes affected by **1** and **2**; B: genes affected by **1** but *not* **2**; C: genes affected by **2** but *not* **1**.

neither **1** nor **2** do repress the entire TNF-α inductome. From the total of 650 up-regulated genes, 67 (10.3%) are repressed by both **1** and **2**, 115 (17.7%) by **1** but not **2**, and 99 (15.2%) by **2** but not **1** at chosen cutoffs. From the set of 650 that were TNF-α–inducible, 369 genes (56.8%) were not affected by either **1** or **2**. The fold changes for the selected genes (Fig. 5) that are induced by TNF-α and affected by **1** are listed in Table 3. Within the subset A, where both **1** and **2** affected gene expression, the most pronounced difference in potency was noted for *IL8* (2.3-fold with the polyamide and 8.4-fold with PS1145). The other four genes experienced comparable down-regulation effects between the polyamide and the kinase inhibitor. Among these is *TNFAIP3*, which plays an essential role in the negative regulation of NF-κB activation (25, 26). Its repression could therefore extend the duration of the NF-κB–mediated signaling cascade.

As for the gene subset B, where **1** but not **2** exhibited substantial gene regulation effects, the most pronounced gene repression was observed with *SERPINE1* (12.7-fold down-regulation upon treatment with **1**). *SERPINE1* (PAI-1) is the principal inhibitor of the tissue-type plasminogen activator and the urokinase-type plasminogen activator (PLAU) and hence an important drug target (27). It plays a pivotal role in inhibiting fibrinolysis and has been implicated in diseases of high impact on the modern society, such as myocardial infarction and atherosclerosis (28, 29). There is evidence for *SERPINE1* expression being regulated by NF-κB, although the exact mechanism of action remains elusive (30). We observe the gene being induced threefold by TNF-α. However, the polyamide treatment results in a thirteenfold repression of the gene, bringing it 4.5-fold below the basal expression level in A549 cells. This observation could either imply constitutive NF-κB–driven expression of the gene or represent an additional manifestation of polyamide off-target effects. The ChIP-seq dataset allowed detecting three NF-κB binding events in the vicinity of the *SERPINE1* transcription start site, on the basis of the established binding motif.* Interestingly, one of the principal protein targets of *SERPINE1*—PLAU—was found to be repressed 5.7-fold by the polyamide at the transcript level. In the gene subset C (Table 3) the kinase inhibitor PS1145 (**2**) had the most pronounced effect on the gene *CCL5*, although **1** did not affect its expression.

Conclusion

We have developed the synthetic polyamide **1** capable of binding the DNA sequences 5′WGGWWW-3′ and 5′GGGWWW-3′. Its activity in cell culture has been assessed by qRT-PCR and RNA-seq, which showed that the molecule affected some 30% of the TNF-α–inducible transcriptome. ChIP experiments conducted on the *IL6* and *IL8* promoters demonstrate that the molecule is capable of reducing the NF-κB promoter occupancy for those genes. The RNA-seq–based comparison between **1** and the established NF-κB inhibitor PS1145 revealed that the two molecules affected a common group of genes but additionally possessed nonoverlapping effects, affecting comparable numbers of genes. From the set of genes affected uniquely by **1**, the strong repression of the *SERPINE1* gene is of potential interest because of the gene's role in myocardial infarction and atherosclerosis. The transcription factor-targeted approach offers an alternative to the existing NF-κB inhibitors and could possess interesting properties for the treatment of inflammatory disorders. Animal model experiments to study the effects of **1** in vivo are under way.

Materials and Methods

Polyamide Synthesis and Characterization. The polyamides **1** and **10** were synthesized by following established solid phase synthesis protocols (31, 32). Binding properties with respect to various DNA sequences were determined by means of DNA thermal denaturation analyses. Cellular uptake was assessed in live A549 cells by using the fluorescein conjugates **3** and **11** in conjunction with confocal microscopy measurements (33). Water-soluble tetrazolium-1 cell proliferation and viability assays were furthermore conducted at different concentrations of **1**. Detailed procedures can be found in *SI Text*.

Gene Expression Analysis by quantitative RT-PCR. Total growth medium was obtained by supplementing F12-K (Gibco) with 10% FBS and 1% penicillin/streptomycin. A549 cells were plated in 12-well plates at a density of 2×10^4 mL^{-1}. The cells were allowed to adhere (16–24 h) and the polyamide **1** subsequently dosed as a DMSO solution at specified concentrations, typically not exceeding 0.2% DMSO final concentration (vol/vol). Untreated reference samples were mock-treated with DMSO at equal volumes. The cells were incubated with **1** for 48 or 72 h or where appropriate with PS1145 for 1.5–2 h and subsequently induced with human recombinant TNF-α (R&D, CF) at 10 ng/mL for 2 or 12 h. The mRNA was extracted by using the QIAGEN® RNeasy mini kit following the standard purification protocol. The mRNA was reverse-transcribed by using the Transcriptor First Strand cDNA Synthesis Kit (Roche). Quantitative PCR was performed by using the FastStart Universal SYBR Green Master (Rox) (Roche) on an ABI 7300 Real Time PCR System. Gene expression was normalized against PPIA and in some cases additionally GUSB as housekeeping genes. All primers yielded single amplicons as determined by both melting denaturation analysis and agarose gel electrophoresis. The following primer pairs were used. *IL6*: *fwd*. 5′-AGT GAG GAA CAA GCC AGA GC *rev*. 5′-GTC AGG GGT GGT TAT TGC AT-3′; *IL8*: fwd. 5′-TCC TGA TTT CTG CAG CTC TGT-3′ *rev*. 5′-AAA TTT GGG GTG GAA AGG TT-3′; PPIA: *fwd*. 5′-CAC CGT GTT CTT CGA CAT TG-3′ *rev*. 5′-TTC TGC TGT CTT TGG GAC CT-3′; GUSB: *fwd*. 5′-CTC ATT TGG AAT TTT GCC GAT T-3′ *rev*. 5′-CCC AGT GAA GAT CCC CTT TTT A-3′.

Chromatin Immunoprecipitation. A549 cells were plated at 3×10^4 mL^{-1} in 500 cm^2 dishes using 100 mL of the cellular suspension per dish. Cells were allowed to adhere to the surface over 16–24 h and subsequently treated with **1** at 10 μM final concentration for 60–70 h. Cell synchronization by FBS starvation (0.5% over 12 h) after polyamide treatment did not change the relative promoter occupancy between the untreated and the polyamide-treated samples. The cells were induced with TNF-α over various time periods, as specified. Cross-linked chromatin was obtained by following established two-step cross-linking protocols (34). The following primer pairs were used. *IL6*: *fwd*. 5′-CCT CAC CCT CCA ACA AAG AT-3′ *rev*. 5′-TTG AGA CTC ATG GGA AAA TCC-3′ (proximal *IL6* promoter; chr7:22,766,715-22,766,767; hg19); *IL8*: *fwd*. 5′-CAT CAG TTG CAA ATC GTG GA-3′ *rev*. 5′-TGC ACC CTC ATC TTT TCA TT-3′ (proximal *IL8* promoter; chr4:74,606,178-74,606,231; hg19). Further specifications of chromatin shearing and isolation procedures can be found in *SI Text*.

ChIP-seq Sample Preparation and Data Processing. Immunoprecipitated DNA samples were combined, typically yielding a total of 5–10 ng. ChIP-seq libraries were prepared by using standard Illumina reagents and protocols. Single read sequencing with the read length of 38 nt was performed on the Illumina GAIIx sequencer by following the manufacturer's instructions, typically producing 25–30 million postfiltered reads per library. The data were processed by employing standard program packages and analytical techniques. See *SI Text* for details on interreplicate reproducibility and NF-κB binding motif statistics (Table S2).

RNA-seq Sample Preparation and Data Processing. Cells were grown as described above, incubated with **1** over 72 h, and subsequently induced with TNF-α for 12 h. Total RNA was isolated by using the TRIzol procedure, yielding 70–100 μg total RNA per condition. The mRNA was enriched for using a double poly-A selection. RNA-seq libraries were prepared by using standard Illumina reagents and protocols. Single read sequencing with the read length of 38 nt was performed on the Illumina GAIIx sequencer by following the manufacturer's instructions, typically producing 25–30 million postfiltered reads per library. The sequencing data were analyzed by using the packages Tophat (mapping against hg19) and Cufflinks (35). All data were processed with the gencode.v4 annotation. See *SI Text* for interreplicate reproducibility (Fig. S7) and data processing thresholds.

ACKNOWLEDGMENTS. Prof. David Baltimore, Dr. Chee-Kwee Ea, and Dr. John W. Phillips are gratefully acknowledged for helpful discussions. J.A.R. is grateful to the Alexander von Humboldt Foundation for the award of a Feodor Lynen postdoctoral fellowship. J.L.M. acknowledges the American Cancer

*chr7:100748247-100748257; chr7:100751724-100751734; chr7:100751938-100751948; *sequences determined as 5′-TGGAATTTCCC-3′(+), 5′-AGGAAAGCCCT-3′ (–) and 5′-GGGGCTTTCCT-3′ (+), respectively.*

Society for a postdoctoral fellowship (PF-10-015-01-CDD). Sequencing was conducted at the Millard and Muriel Jacobs Genetics and Genomics Laboratory at California Institute of Technology. This work was supported by The Ellison Medical Foundation (Grant AG-SS-2256-09).

1. Grivennikov SI, Greten FR, Karin M (2010) Immunity, inflammation, and cancer. *Cell* 140:883–899.
2. Karin M, Cao YX, Greten FR, Li ZW (2002) NF-kappa B in cancer: From innocent bystander to major culprit. *Nat Rev Cancer* 2:301–310.
3. Kawahara TLA, et al. (2009) SIRT6 links histone H3 lysine 9 deacetylation to NF-kappa B-dependent gene expression and organismal life span. *Cell* 136:62–74.
4. Sen R, Baltimore D (1986) Multiple nuclear factors interact with the immunoglobulin enhancer sequences. *Cell* 46:705–716.
5. Gilmore TD (2006) Introduction to NF-kappa B: Players, pathways, perspectives. *Oncogene* 25:6680–6684.
6. Gilmore TD, Herscovitch M (2006) Inhibitors of NF-kappa B signaling: 785 and counting. *Oncogene* 25:6887–6899.
7. Dervan PB, Edelson BS (2003) Recognition of the DNA minor groove by pyrrole-imidazole polyamides. *Curr Opin Struct Biol* 13:284–299.
8. Hsu CF, et al. (2007) Completion of a programmable DNA-binding small molecule library. *Tetrahedron* 63:6146–6151.
9. Kielkopf CL, et al. (1998) A structural basis for recognition of A.T and T.A base pairs in the minor groove of B-DNA. *Science* 282:111–115.
10. White S, Szewczyk JW, Turner JM, Baird EE, Dervan PB (1998) Recognition of the four Watson-Crick base pairs in the DNA minor groove by synthetic ligands. *Nature* 391:468–471.
11. Chenoweth DM, Dervan PB (2009) Allosteric modulation of DNA by small molecules. *Proc Natl Acad Sci USA* 106:13175–13179.
12. Olenyuk BZ, et al. (2004) Inhibition of vascular endothelial growth factor with a sequencespecific hypoxia response element antagonist. *Proc Natl Acad Sci USA* 101:16768–16773.
13. Nickols NG, Jacobs CS, Farkas ME, Dervan PB (2007) Modulating hypoxia-inducible transcription by disrupting the HIF-1-DNA interface. *ACS Chem Biol* 2:561–571.
14. Nickols NG, Dervan PB (2007) Suppression of androgen receptor-mediated gene expression by a sequence-specific DNA-binding polyamide. *Proc Natl Acad Sci USA* 104:10418–10423.
15. Muzikar KA, Nickols NG, Dervan PB (2009) Repression of DNA-binding dependent glucocorticoid receptor-mediated gene expression. *Proc Natl Acad Sci USA* 106:16598–16603.
16. Wurtz NR, Pomerantz JL, Baltimore D, Dervan PB (2002) Inhibition of DNA binding by NF-κB with pyrrole-imidazole polyamides. *Biochemistry* 41:7604–7609.
17. Chenoweth DM, Poposki JA, Marques MA, Dervan PB (2007) Programmable oligomers targeting 5′-GGGG-3′ in the minor groove of DNA and NF-κB binding inhibition. *Bioorg Med Chem* 15:759–770.
18. Matsuda H, et al. (2011) Transcriptional inhibition of progressive renal disease by gene silencing pyrrole-imidazole polyamide targeting of the transforming growth factor-beta 1 promoter. *Kidney Int* 79:46–56.
19. Kasowski M, et al. (2010) Variation in transcription factor binding among humans. *Science* 328:232–235.
20. Kannabiran C, Zeng X, Vales LD (1997) The mammalian transcriptional repressor RBP (CBF1) regulates interleukin-6 gene expression. *Mol Cell Biol* 17:1–9.
21. Kunsch C, Lang RK, Rosen CA, Shannon MF (1994) Synergistic transcriptional activation of the IL-8 gene by NF-kappa B p65 (RelA) and NF-IL-6. *J Immunol* 153:153–164.
22. Lam LT, et al. (2005) Small molecule inhibitors of I kappa B kinase are selectively toxic for subgroups of diffuse large B-cell lymphoma defined by gene expression profiling. *Clin Cancer Res* 11:28–40.
23. Verstrepen L, et al. (2008) TLR-4, IL-1R and TNF-R signaling to NF-kappa B: Variations on a common theme. *Cell Mol Life Sci* 65:2964–2978.
24. Chen FE, Huang DB, Chen YQ, Ghosh G (1998) Crystal structure of p50/p65 heterodimer of transcription factor NF-κB bound to DNA. *Nature* 391:410–413.
25. Vereecke L, Beyaert R, van Loo G (2009) The ubiquitin-editing enzyme A20 (TNFAIP3) is a central regulator of immunopathology. *Trends Immunol* 30:383–391.
26. Vereecke L, et al. (2010) Enterocyte-specific A20 deficiency sensitizes to tumor necrosis factor-induced toxicity and experimental colitis. *J Exp Med* 207:1513–1523.
27. Sprengers ED, Kluft C (1987) Plasminogen-activator inhibitors. *Blood* 69:381–387.
28. Eriksson P, Kallin B, Vanthooft FM, Bavenholm P, Hamsten A (1995) Allele-specific increase in basal transcription of the plasminogen-activator inhibitor-1 gene is associated with myocardial infarction. *Proc Natl Acad Sci USA* 92:1851–1855.
29. Schneiderman J, et al. (1992) Increased type-1 plasminogen-activator inhibitor gene expression in atherosclerotic human arteries. *Proc Natl Acad Sci USA* 89:6998–7002.
30. http://www.nf-kb.org/.
31. Belitsky JM, Nguyen DH, Wurtz NR, Dervan PB (2002) Solid-phase synthesis of DNA binding polyamides on oxime resin. *Bioorg Med Chem* 10:2767–2774.
32. Nickols NG, Jacobs CS, Farkas ME, Dervan PB (2007) Improved nuclear localization of DNA-binding polyamides. *Nucl Acids Res* 35:363–370.
33. Edelson BS, et al. (2004) Influence of structural variation on nuclear localization of DNA-binding polyamide-fluorophore conjugates. *Nucl Acids Res* 32:2802–2818.
34. Nowak DE, Tian B, Brasier AR (2005) Two-step cross-linking method for identification of NF-κB gene network by chromatin immunoprecipitation. *BioTechniques* 39:715–725.
35. Trapnell C, et al. (2010) Transcript assembly and quantification by RNA-Seq reveals unannotated transcripts and isoform switching during cell differentiation. *Nat Biotechnol* 28:511–515.